Journal of
Materials Chemistry A

Desensitization of the dinitromethyl group: molecular/crystalline factors that affect the sensitivities of energetic materials

Journal Name

ARTICLE

Desensitization of the dinitromethyl group: molecular/crystalline factors that affect the sensitivities of energetic materials

Jichuan Zhang[a,b,c], Jiaheng Zhang*[a,b], Damon A. Parrish[d], and Jean'ne M. Shreeve*[c]

The dinitromethyl group has attracted considerable attention because of its high nitrogen and oxygen content, positive oxygen balance and high energy. Although most dinitromethyl-functionalized compounds suffer from sensitivity to mechanical stimuli, a series of 3-dinitromethanide-1,2,4-triazolone-based energetic salts were now synthesized and fully characterized. Of these, the ammonium salt is insensitive to impact and friction. X-ray single crystal analysis shows that the ammonium moiety arranges through a close layer-by-layer assembly, which is helpful in decreasing sensitivity. In addition, intramolecular hydrogen-bonding interactions, and intense π-π interactions also are stabilizing factors which impact the sensitivity of the ammonium salt. The enthalpies of formation and energetic properties of the series of salts were determined in order to reach the conclusion that these multiple stabilization factors are effective tools in decreasing the sensitivity of dinitromethyl-based energetic materials.

Introduction

Since Alfred Nobel paved the way to the development of dynamite, energetic materials have drawn extensive interest and have been widely used in both military and civilian applications,[1] such as gas generating agents suitable for airbags,[2,3] propellants as fuel for rockets,[4-7] and explosives for bombs and mines.[8-13] For modern energetic compounds, insensitivity and excellent detonation properties are two very important characteristics that are contradictory in nature; hence, achieving a fine balance between low sensitivity and high energetic performance is a huge challenge. However, a few instances exist which combine insensitivity and high energetic performance successfully, such as TATB, LLM-116 and LLM-105 (Scheme 1),[14-19] inspiring us to further explore excellent insensitive materials with high energy.
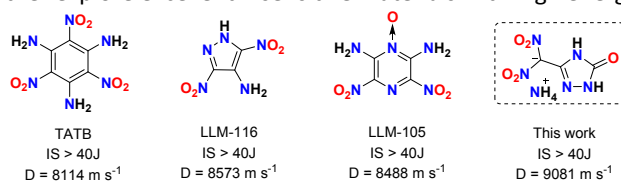
Scheme 1. Several classical high-energy-insensitive compounds

Azole-based energetic materials have aroused enormous attention because of the relatively high heats of formation and friendly environment upon decomposition.[20] Triazole-based energetic materials, combine heats of formation, energetic properties, and sensitivity in a fine balance,[21] for example, 3,3′-dinitro-5,5′-bis-1,2,4-triazole-1,1′-diol and its derivatives[22] and 5-nitro-3-trinitromethyl-1H-1,2,4-triazolate derivatives.[23,24] Since the excellent energetic properties of these materials are generally superior to those of RDX and comparable to HMX, they are attractive for development as modern energetic compounds.

Dinitromethyl is a promising energetic group owing to its high nitrogen and oxygen content, which often leads to high energy density for dinitromethyl-functionalized compounds including an acceptable oxygen balance.[25,26] However, most of the dinitromethyl-based compounds are sensitive to mechanical stimulus. For instance, 2-dinitromethyl-5-nitrotetrazole[27] and dihydroxylammonium 3-dinitromethyl-4-nitraminofurazan,[28] detonation velocities and pressures are 9.22 km s^{-1}, 9.65 km s^{-1} and 38.5 Gpa, 43 Gpa, respectively. At the same time, the impact and friction sensitivities of these two compounds are 5, 8J and 80, 64N, respectively. According to the standard,[29] these two representatives fall in the extremely sensitive level, which seriously limits their potential applications. Hence, to make functionalized compounds which are insensitive to mechanical stimulus, use of such an excellent and attractive energetic moiety is an exciting challenge. Our group recently proposed enforced layer-by-layer stacking, which can decrease sensitivity effectively.[30] Additionally, intramolecular hydrogen-bonds also play a significant role in improving stability.[31,32] In our continuing efforts,[33] enforced layer-by-layer stacking and intramolecular hydrogen bonding interactions were combined extensively in the

a. State Key Laboratory of Advanced Welding and Joining, Harbin Institute of Technology, Shenzhen, 518055, China.
b. Research Centre of Flexible Printed Electronic Technology, Harbin Institute of Technology, Shenzhen, 518055, China
c. Department of Chemistry, University of Idaho, Moscow, Idaho 83844-2343, United States
d. Naval Research Laboratory, 4555 Overlook Avenue, Washington, D.C. 20375, United States

crystals of ammonium 3-dinitromethanide-1,2,4-triazolone (**2**). A large number of O-H weak interactions and intense π-π interactions were also found in the crystals of **2**. Overall, these positive factors led to the insensitivity of **2** towards impact and friction, which is remarkably less sensitive than other 3-dinitromethanide-1,2,4-triazolone-based compounds.

Results and discussion

Synthesis and Single Crystal X-ray Structures.

Compound **1** and its silver salt were prepared according to the procedure described in our earlier work.[33] Compounds **2**, **4**, **7**-**12** were obtained through the reaction of **1** and free bases, and aqueous ammonia. Compounds **5** and **6** were obtained through the reaction of the silver salt of **1** and the chlorides of **5**, and **6**, respectively (Fig. 1).

Crystals of **2**, **5·H₂O**, and **6** are suitable for single-crystal X-ray diffraction; all of them were crystallized from the mixture of ethanol and water. Ammonium 3-dinitromethanide-1,2,4-triazolone (**2**) crystallizes in the triclinic space group P-1 (2), with two 3-dinitromethanide-1,2,4-triazolone anions and two ammonium ions in each lattice cell (Z = 2, Fig. 2a). The density of **2** is 1.86 cm^{-3} at 150K which approaches the highest densities of any known dinitromethyl-based ammonium salts. The ammonium ions and the corresponding anions are coplanar and form a layer-by-layer stacking structure. In addition, a large number of intramolecular hydrogen bonds form among the ammonium ions, triazole rings, and dinitromethyl groups. The lengths of the hydrogen bonds (O/N…H) range from 1.86 Å to 2.12 Å, falling within the normal hydrogen bonding range. The distance between the two triazolone centroids is 3.247 Å (Fig. 2b), which is less than 4.0 Å, suggesting that two of the 3-dinitromethanide-1,2,4-triazolone anions are in the range of π-π interactions and the triazolone ring from above is stacked close to the dinitromethyl group from below. In other words, the arrangement of anions and cations crystalizes face-to-face. The layer arrangement of 3-dinitromethanide-1,2,4-triazolone anions and ammonium cations is connected through hydrogen bonds and π-π interactions forming a 3-D net structure (Fig. 2c).
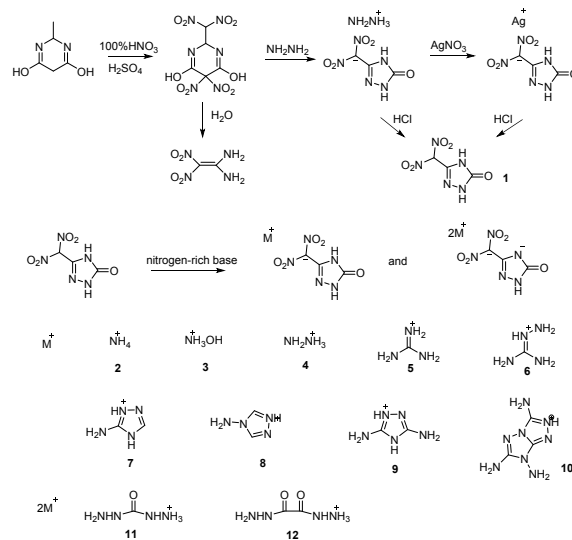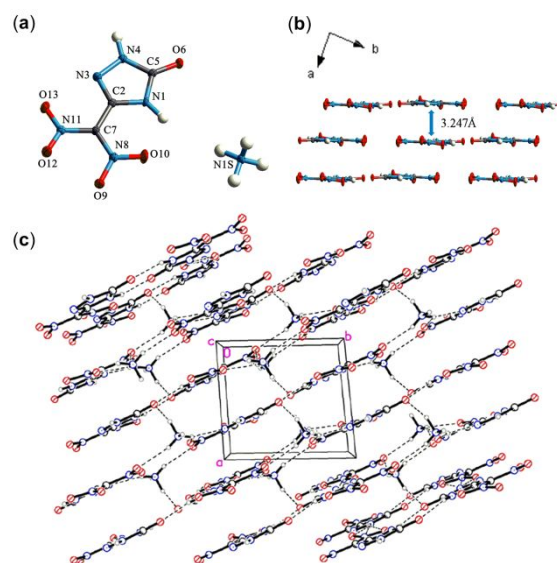

Fig 1. Synthesis route of 3-dinitromethanide-1,2,4-triazolone-based compounds

Fig 2. (a) Single-crystal X-ray structure of **2**; (b) edge-to-face π-π stacking of triazolone rings; (c) Intermolecular hydrogen bonds and unit cell view along the c axis

Monohydrate guanidinium 3-dinitromethanide-1,2,4-triazolone (**5·H₂O**) is a yellow block crystal which crystallizes in the triclinic space group P-1 (2), with two 3-dinitromethanide-1,2,4-triazolone anions, two water molecules, and two guanidinium ions in each lattice cell (Z = 2) (Fig. 3a). The density of **5·H₂O** is 1.754 g cm^{-3} at 150 K. Similar to **2**, the 3-dinitromethanide-1,2,4-triazolone anion, water molecule, and guanidinium cation are coplanar, and the crystal also crystallizes in the form of layer-by-layer stacking. The distance between the
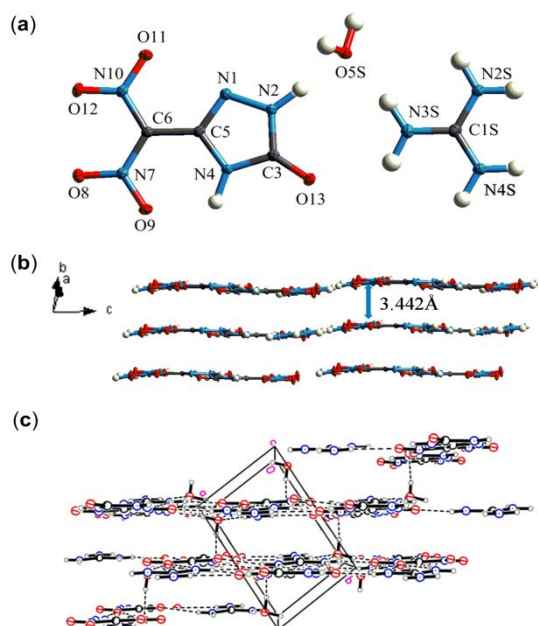
Fig 3. (a) Single-crystal X-ray structure of **5**·H₂O; (b) layer-by-layer stacking of **5**; (c) unit cell and intermolecular hydrogen bonds of **5**.
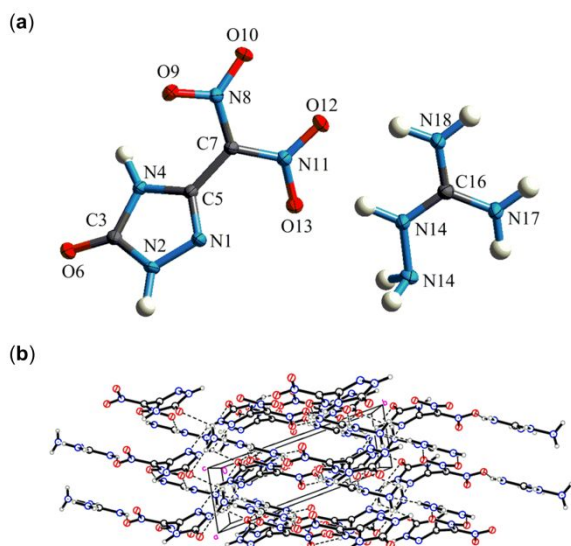

Fig 4. (a)Single-crystal X-ray structure of **6**; (b) crystal stacking of **6**

two centroids of triazolone is 3.442 Å (Fig. 3b), which is also in the range of π-π interactions, and the 3-dinitromethanide-1,2,4-triazolone anion, water molecule, and guanidinium cation are extensively connected by hydrogen bonds (Fig. 3c). The lengths of hydrogen bonds (O/N···H) are in the range of 1.804 to 2.389 Å.

Aminoguanidinium 3-dinitromethanide-1,2,4-triazolone (**6**) crystallizes in the same space group as **2** (Fig. 4a), with a density of 1.77 g cm⁻³ at 150 K. The dinitromethyl and the diaminoguanidinium groups are in the same plane due to hydrogen bonding interactions. The volume of the diaminoguanidinium cation is larger than the guanidinium and

ammonium cations, leading to the compression of the arrangement space; hence, the torsion angle between the triazolone and the dinitromethyl groups is 43.05°, and the 3-D network of the crystal results through hydrogen bonding (Fig. 4b).

Thermal stability and sensitivity

In general, thermal stability is a primary concern since an unacceptably low decomposition temperature will strictly limit applications of the energetic material. Differential scanning calorimetric (DSC) measurements were performed on all the compounds at a scanning rate of 5 °C min⁻¹, and comparison of the decomposition results with that of the parent compound (Td: 127 °C, Table 1) shows that all of the salts are more stable thermally. Compound **2** has an onset decomposition temperature of 166 °C, which is consistent with its hydroxylammonium salt. For compounds **4**, **5**, and **10**, decomposition temperatures are 184, 178, and 213 °C, respectively (Table 1). Addition to the intramolecular hydrogen-bonding plays an important role in improving the stabilities of these salts. The bond dissociation energy between anions and cations also plays a significant role in enhancing their thermal stabilities because the bond dissociation energies in salts are usually higher relative to their precursors[20].

Sensitivities are crucial in the evaluation of the safety characteristics of energetic materials during manufacturing,
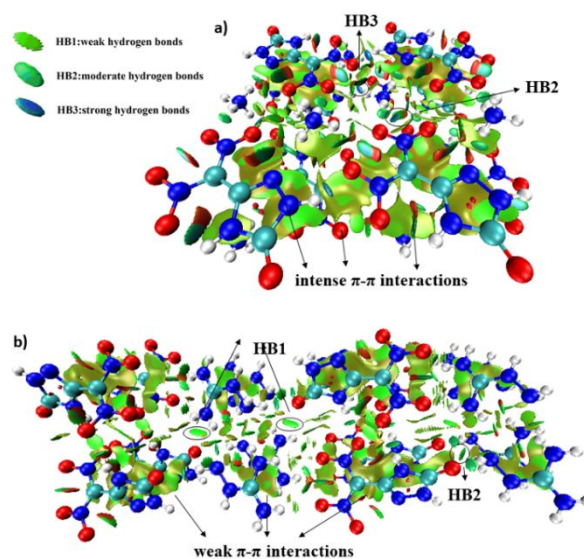

Fig 5. NIC plots of gradient isosurfaces (s = 0.5 au) for **2** (a) and **6** (b) unit cells. The geometries of the unit cells were optimized at the BLYPD3/def2-QZVPP method 32 using ORCA 3.0.33 The surfaces are colored on a blue-green-red scale indicating strong attractive interactions, weak attractive, and strong nonbonded overlap, respectively.

applications, and transportation. The experimental impact and friction sensitivity values were determined with standard BAM drop hammer and friction tester techniques. Among these synthesized 3-dinitromethanide-1,2,4-triazolone-based salts,
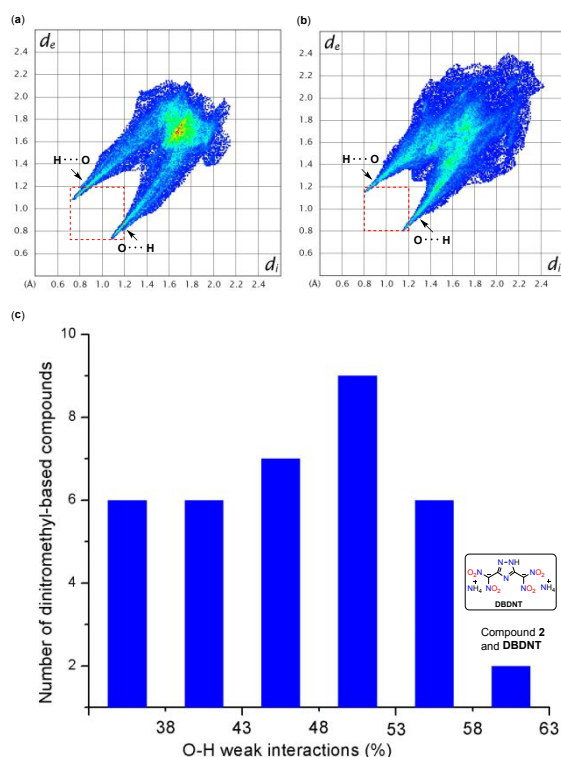
Fig 6. a) Weak interactions of **2**; b) Weak interactions of DBDNT; c) The strength distribution statistics of total O-H weak interactions.

the ammonium salt of 3- dinitromethanide-1,2,4-triazolone is insensitive to impact and friction (Table 1), it shows comparable sensitivities to TATB and LLM-116, which further highlights its potential applications. The insensitivity of **5**·H_2O to mechanical stimuli may be the result of the water molecule of crystallization. Except for **4**, the impact sensitivities of all the remaining 3-dinitromethanide-1,2,4-triazolone salts are between 32 and 35 J. All of these salts are insensitive towards friction

(>360N) and are remarkably less sensitive than their precursor (22 J, 240 N) on impact and friction to stimuli.

Theoretically, any external mechanical force acting on an energetic material can lead to a certain deformation to produce strain and store mechanical energy which results in many "hotspots" during this progress. When the temperature of these "hotspots" becomes higher than the decomposition temperature of the material, decomposition or explosion may be activated.[34] In general, the arrangement of these energetic molecules or ions are classified into four categories,[31] namely (1) layer assembly; (2) wavelike; (3) crossing; and (4) mixing, respectively. Among these, the layer assembly is the desirable arrangement for energetic constituents since the layer assembly geometries of energetic materials can absorb mechanical stimuli by converting kinetic energy into layer sliding which results in lower sensitivity.[33]

To gain further information about inter- and intramolecular effects and comprehensively study their influence on crystal packing, as well as sensitivities associated with 2 and other 3-dinitromethanide-1,2,4-triazolone salts, the non-covalent interaction (NCI) plot was applied to analyze real space structure based on electron density.[34] The calculated results based on this simple theory indicate that the interlayer π–π interactions are more intense and spread over a larger area in **2** compared to that of **6**, which can be easily observed as large green isosurfaces (Fig. 5). In addition, the shape of hydrogen bonding (HB) in the NCI plot can be characterized by the small, ellipse shaped surfaces which, in theory, are large accumulations of electron density. In contrast to **6**, more extensive HB interactions were observed in layered **2**. Hence, more intensive π–π interactions and hydrogen bonding of the layer-by-layer stacking, these positive factors result in 2 being insensitive to impact and friction.

In addition to the closer layer-by-layer packing, the weak interactions, which primary consist of O-H 'soft' interactions, play a significant role in the sensitivity of energetic materials. In this study, Hirschfeld surfaces[36] were employed to analyse the weak interactions of compounds **2**, **5**, and **6** (Fig. 6 and 7), and further to examine up to 33 dinitromethyl-functionalized CIFs[27,28,33,37-42] from the Cambridge Structural Database.

Table 1. Physical properties of compound 2 and 4-12

Comp	T_d[a] °C	ρ [b] [g cm^{-3}]	$-\Delta_f H$ [c] [kJ mol^{-1} /kJ g^{-1}]	D[d] [m s^{-1}]	P[e] [Gpa]	IS[f] (J)	FS[g] (N)
2	166	1.85	174/0.84	9081	37.0	>40	>360
4	184	1.88	128/0.58	9226	37.4	26	240
5	178	1.74	194/0.78	7989	24.2	>40	>360
6	155	1.77	83/0.31	8594	28.9	33	>360
7	150	1.76	43.9/0.16	8111	25.9	32	>360
8	148	1.74	170.9/0.46	8182	26.4	32	>360
9	170	1.78	8.6/0.03	8201	26.2	32	>360

10	213	1.86	729.2/2.12	9108	34.0	35	>360
11	144	1.84	118.4/0.32	9196	33.6	34	>360
12	154	1.84	14.4/0.03	8879	31.9	34	>360
TATB	360	1.93	-154.2/-0.60	8114	31.2	>40	>360
RDX	205	1.81	80/0.36	8795	34.9	7.4	120
HMX	280	1.91	104.8/0.36	9144	39.2	7.4	120
LLM-116	178	1.90	96.3/0.56	8573	34.2	>40	>360

[a] Decomposition temperature (onset). [b] Density measured by gas pycnometer (25 °C). [c] Heat of formation. [d] Detonation velocity (calculated with Explo5 v6.01).[e] Detonation pressure (calculated with Explo5 v6.01). [f] Impact sensitivity. [g] Friction sensitivity.
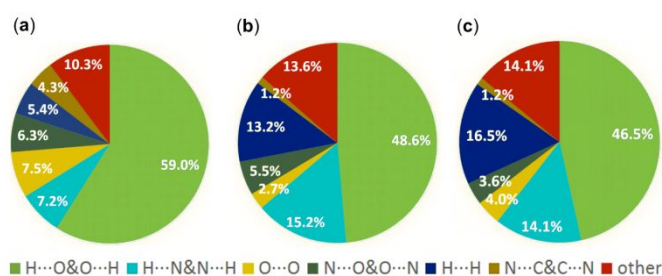

Fig 7. Pie graphs of individual atomic contacts percentage contribution to the Hirshfeld surfaces for **2** (a), **5** (b), and **6** (c).

We found that among these 36 dinitromethyl-functionalized energetic compounds, **2** has the second highest percentage of O-H weak interactions, possessing 59%. Although the percentage of O-H weak interactions of **2** is slightly lower than that of the DBDNT (diammonium 3,5-bis(dinitromethyl)- 1,2,4-triazolate), interactions (indicated by the location and size of the red square frame) in **2** are apparently higher than that of the DBDNT. Furthermore, from the pie graphs of individual atomic contacts percentage contributions, it is seen that the percentage of C-N and N-C weak interactions of **2** is 4.3% which is the highest value of all the 3-dinitromethanide-1,2,4-triazolone-based compounds, suggesting again that there exists powerful π-π interactions in **2** between the two adjacent triazole rings (Fig. 7) Therefore, the closer layer-by-layer package, multi intramolecular hydrogen-bonding interactions, and second highest and relatively stronger O-H weak interactions as well as extensive π-π interactions, all contribute to the insensitivity of **2**.

Density and Detonation Properties.

At ambient temperature, the densities of **2** and **4**-**12** fall between 1.73 g cm^{-3} and 1.90 g cm^{-3}. The densities of **2**, **4**, **8**, **10** and **12** are equal to or greater than 1.80 g cm^{-3}, belonging to the class of high density energetic materials (HEDM). Compounds **2** and **4** have densities of 1.85 and 1.88 g cm^{-3}, respectively, which are only rarely reported for dinitromethyl-based energetic ammonium and diaminoguanidinum salts.

Based on the calculated heats of formation, detonation properties of all the new compounds were determined by EXPLO5 (6.01). As shown in Table 1, all the dinitromethyl-functionalized energetic salts have excellent detonation performance. The detonation velocity and pressure of **2** are 9081 m s^{-1} and 37.0 Gpa, superior to TATB at the same level of sensitivity, suggesting its promising applications as a candidate to replace TATB. Compounds **4**, **10** and **11** possess higher detonation velocities and pressures (**4**： D = 9226 m s^{-1}, P = 37.4 Gpa; **10**: D= 9108 m s^{-1}, P = 34.0 Gpa; **11**: D = 9196 m s^{-1}, P=33.6 Gpa, respectively) than those of RDX, and detonation velocities comparable to those of HMX. Moreover, these compounds exhibit lower sensitivities than RDX and HMX, indicating that they are the potential candidates for applications that require such properties.

Conclusions

In summary, the ammonium salt of dinitromethanide-1,2,4-triazolone (**2**) crystallizes with close layer-by-layer stacking, which plays a positive role in decreasing sensitivity. In addition, intramolecular hydrogen-bonding interactions, second highest (possessing 59%) and relatively stronger O-H weak interactions, as well as powerful π-π interactions together result in the insensitivity of **2** towards mechanical stimuli which makes it remarkably less sensitive than other 3-dinitromethanide-1,2,4-triazolone-based compounds. The detonation velocity and pressure of **2** are 9081 m s^{-1} and 37.0 Gpa, respectively - superior to TATB. This indicates that **2** may be a potential replacement of TATB. In addition, the detonation performance of **4** ,**10** and **11** (**4** ： D = 9226 m s^{-1}, P = 37.4 Gpa; **10**: D = 9108 m s^{-1}, P = 34.0 Gpa; **11**: D = 9196 m s^{-1}, P = 33.6 Gpa, respectively) are superior to those of RDX and detonation velocities are comparable to HMX, and are less sensitive to impact and friction than those of RDX and HMX, suggesting that these compounds could act as potential candidates with decreased sensitivity and high performance. Overall, through utilization of these stable factors, dinitromethyl-based energetic materials can become insensitive, and these findings may be a promising tool to design high energy insensitive materials.

Experimental

Safety Precautions.

Although we experienced no difficulties in synthesis and characterization of these materials, proper protective procedures should be followed. All the reactions were carried out in a hood behind a safety shield and face shield, and leather gloves were worn at all times. Caution was exercised at all times during the synthesis, characterization, and handling of any of these materials.

Materials and Methods.

Commercial analytical grade reagents were used without further purification. ^{1}H and ^{13}C spectra were recorded on a 300 MHz (Bruker AVANCE 300) nuclear magnetic resonance spectrometer operating at 300.13 and 75.48 MHz, respectively. A 500 MHz (Bruker AVANCE 500) nuclear magnetic resonance spectrometer operating at 50.69 MHz was used to obtain ^{15}N spectra for **2**. Chemical shifts in the 1H and 13C spectra are reported relative to Me_4Si and ^{15}N NMR to $MeNO_3$. DFT and ab initio calculations were carried out using the Gaussian 09 program package.[43] The NCIs plots were calculated using Multiwfn[44] and visualized by VMD program.[45] Hirshfeld surfaces and associated 2D fingerprints were generated by CrystalExplorer 3.1.25.[46]The X-ray intensity data were measured on a Bruker Apex 2 CCD system equipped with a graphite monochromator and a Mo−Kα fine focus tube (λ = 0.71073 Å). An Oxford Cobra low-temperature device was used to maintain low temperatures. The melting and decomposition (onset) points were obtained on a differential scanning calorimeter (TA Instruments Co., model Q10) at the scan rate of 5 **°C** min^{-1}. Densities were measured at room temperature using a Micromeritics AccuPyc 1330 gas pycnometer. The impact and friction-sensitivity measurements were conducted by employing a standard BAM Fallhammer and a BAM friction tester.

X-ray Crystallography.

A yellow block crystal of dimensions 0.095 × 0.063 × 0.028 mm^3 for **2**, a faint yellow block crystal of dimensions 0.44 × 0.21 × 0.04 mm^3 for **5** and a yellow needle crystal of dimensions 0.10 × 0.08 × 0.02 mm^3 for **6** were used for the X-ray crystallographic analysis. The X-ray intensity data were measured on a Bruker Apex 2 CCD system equipped with a graphite monochromator and a Mo−Kα fine focus tube (0.71073 Å). An Oxford Cobra low-temperature device was used to maintain low temperatures. The frames were integrated with the Bruker SAINT Software package using a narrow-frame algorithm and data were corrected for absorption effects using the multiscan method (SADABS).[47]The structures were solved and refined using the Bruker SHELXTL[48]Software Package.

Syntheses

General procedure for the preparation of salts 2, 4, 7, 8, 9 and 10.

Compound **1** (0.378g, 2 mmol) was added to ethanol (20 mL) with stirring. The free base (2 mmol) of aqueous ammonia (25%), hydrazine hydrate (80%), and the neutral compounds of **7**-**10** were added to the ethanol solution, respectively. The reaction mixture was stirred at room temperature for 30 min followed by standing for 3 h. The precipitate was collected by filtration and washed with small amounts of ethanol (5 x 2 mL) to give the products after air drying.

General procedure for the preparation of salts 5 and 6.

To a stirring solution of the silver salt of **1** (590 mg, 2.0 mmol) in water (10 mL), were added chlorides of **5** (191 mg, 2 mmol) or **6** (221 mg, 2

mmol), respectively. Then, the reaction mixture was stirred at room temperature for 30 min followed by standing for 3 h. The filtrate was evaporated in vacuo; the solid residue was recrystallized from methanol and dried.

General procedure for the preparation of salts 5 and 6.

Compound **1** (0.378 g, 2 mmol) was added to the ethanol with stirring and the free base (4 mmol) of **11** and **12** were added to the ethanol solution, respectively. The reaction mixture was stirred at room temperature for 30 min followed by standing for 3 h. The precipitate was collected by filtration and washed with small amount of ethanol to give the products after air drying.

Ammonium 3-dinitromethanide-1,2,4-triazolone (2). Yellow solid (0.84 g, 95%); ^{1}H NMR (DMSO-d6): δ 11.2 (s, 1H), 11.5 (s, 1H), 7.0-7.3 (t, 4H) ppm; ^{13}C NMR (DMSO-d6): δ 156.2, 139.5, 124.6 ppm; ^{15}N NMR (DMSO-d6): δ −21.9, −112.2, 210.8, 212.9, 236.7, 358.3 ppm; IR (KBr): ṽ 3064, 1692, 1545, 1481,1449, 1351, 1222, 1215, 1150, 1065, 1036, 955, 802, 760, 739, 548 cm^{-1}; elemental analysis, Calcd (%) for $C_3H_6N_6O_5$ (206.04): C: 17.48; H: 2.93; N: 40.77; Found, C: 17.29; H: 2.66; N: 40.55.

Hydrazinium 3-dinitromethanide-1,2,4-triazolone (4). Yellow solid (0.84 g, 95%); ^{1}H NMR(DMSO-d6): δ 11.4 (s, 1H), 11.1 (s, 1H), 9.95 (s, 5H) ppm; ^{13}C NMR (DMSO-d6): δ 155.9, 139.4, 124.4 ppm; ^{15}N NMR (DMSO-d6): δ −21.9, −112.2, −210.9, -212.8, -217.0, −237.4, −331.6 ppm; IR (KBr): ṽ 3343, 3287, 3074, 2992, 2887, 1725, 1628, 1575, 1508, 1250, 1140, 1102, 1080, 966, 746 cm^{-1}; elemental analysis, Calcd (%) for $C_3H_7N_7O_5$ (221.13): C: 16.29; H: 3.19; N: 44.34; Found, C: 16.19; H: 3.16; N: 43.89.

Guanidinium 3-dinitromethanide-1,2,4-triazolone (5). Yellow solid (0.84 g, 95%); ^{1}H NMR(DMSO-d6): δ 11.1 (br, 2H), 7.0 (br, 6H) ppm; ^{13}C NMR (DMSO-d6): δ 157.9, 156.5, 140.0, 124.7 ppm; IR (KBr): ṽ 3466, 3414, 3349, 3269, 3206, 1723, 1647, 1494, 1452, 1361, 1219, 1134, 1072, 962 cm^{-1}; elemental analysis, Calcd (%) for $C_4H_8N_8O_5$ (248.16): C: 19.36; H: 3.25; N: 45.15; Found, C: 19.15; H: 3.13; N: 44.40.

Aminoguanidinum 3-dinitromethanide-1,2,4-triazolone (6). Yellow solid (0.84 g, 95%); ^{1}H NMR (DMSO-d6): δ 11.4 (s, 1H), 11.1 (s, 1H), 8.54 (s, 1H), 6.7-7.2 (br, 4H), 4.67 (s, 2H) ppm; ^{13}C NMR (DMSO-d6): δ 158.8, 156.0, 139.4, 124.4 ppm; ^{15}N NMR(DMSO-d6): δ −21.9, −112.2, -112.4, -211.0, -213.0, −236.5, -238.5, -282.5, 284.4 ppm; IR (KBr): ṽ 3426, 3343, 3226, 1740, 1665, 1506, 1448, 1393, 1233, 1138, 1072, 1033, 962 cm^{-1}; elemental analysis, Calcd (%) for $C_4H_9N_9O_5$ (263.17): C: 18.26; H: 3.45; N: 47.90; Found, C: 17.98; H: 3.45; N: 47.28.

3-Amino-1,2,4-triazolium 3-dinitromethanide-1,2,4-triazolone (7). Yellow solid (0.84 g, 95%); ^{1}H NMR (DMSO-d6): δ 11.4 (s, 1H), 11.1 (s, 1H), 7.8 (s, 1H), 7.5 (s, 2H), 5.9 (s, 1H) ppm; ^{13}C NMR (DMSO-d6): δ 171.4, 156.0, 153.1, 139.4, 124.4 ppm; IR (KBr): ṽ 3356, 3139, 1708, 1558, 1499, 1309, 1198, 1004, 731 cm^{-1}; elemental analysis, Calcd (%) for $C_5H_7N_9O_5$ (273.17): C: 21.76; H: 2.55; N: 46.75; Found, C: 22.10; H: 2.59; N: 47.75.

4-Amino-1,2,4-triazolium 3-dinitromethanide-1,2,4-triazolone (8). Yellow solid (0.84 g, 95%); ^{1}H NMR (DMSO-d6): δ 11.4 (s, 1H), 11.1 (s, 1H), 9.74 (br, 2H), 8.7 (s, 1H), 6.0 (br, 2H) ppm; ^{13}C NMR (DMSO-d6): δ 156.0, 144.0, 139.3, 124.3 ppm; IR (KBr): ṽ 3337, 3240, 3124, 1690, 1548, 1483, 1376, 1296, 1222, 1136, 1107, 993 cm^{-1}; elemental analysis, Calcd (%) for $C_5H_7N_9O_5$ (273.17): C: 21.98; H: 2.58; N: 46.15; Found, C: 22.00; H: 2.52; N: 45.95.

3,5-Diamino-1,2,4-triazolium 3-dinitromethanide-1,2,4-triazolone (9). Yellow solid (0.84 g, 95%); ^{1}H NMR (DMSO-d6): δ 11.4 (s, 1H), 11.1 (s, 1H), 8.8 (s, 1H), 7.3 (s, 4H) ppm; ^{13}C NMR (DMSO-d6): δ 159.4, 156.7,

140.3, 124.4 ppm; IR (KBr): ṽ 3325, 3157, 1700, 1656, 1611, 1574, 1490, 1385, 1325, 1032, 1009, 937, 728 cm^{-1}; elemental analysis, Calcd (%) for $C_5H_8N_{10}O_5$ (288.18): C: 20.84; H: 2.80; N: 48.60; Found, C: 20.59; H: 2.60; N: 48.35.

3,6,7-Triamino-[1,2,4]triazolo[4,3-b][1,2,4]triazolium 3-dinitromethanide-1,2,4-triazolone (10). Yellow solid (0.84 g, 95%); ^{1}H NMR (DMSO-d6): δ 11.4 (s, 2H), 11.2 (s, 1H), 8.1 (s, 2H), 7.2 (s, 2H), 5.7 (s, 2H) ppm; ^{13}C NMR(DMSO-d6): δ 160.1, 156.0, 147.5, 141.3, 139.5, 124.4 ppm; IR (KBr): ṽ 3455, 3354, 3288, 3234, 3153, 1690, 1653, 1551, 1475, 1410, 1275, 1250, 1140, 1041, 760, 729 cm^{-1}; elemental analysis, calcd (%) for $C_6H_9N_{13}O_5$ (345.24): C: 21.00; H: 2.64; N: 53.05; Found, C: 20.55; H: 2.60; N: 52.26.

Carbohydrazide 3-dinitromethanide-1,2,4-triazolone (11). Yellow solid (0.84 g, 95%); ^{1}H NMR (DMSO-d6): δ 11.4 (br, 1H), 11.1 (br, 1H), 8.0 (br, 10H) ppm; ^{13}C NMR (DMSO-d6): δ 158.7, 155.9, 139.4, 124.4 ppm; IR (KBr): ṽ 3346, 3113, 1663, 1570, 1480, 1460, 1213, 1136, 1068, 978, 798, 761 cm^{-1}; elemental analysis, Calcd (%) for $C_5H_{15}N_{13}O_7$ (369.26): C: 16.26; H: 4.09; N: 49.31; Found, C: 16.11; H: 4.09; N: 49.04.

Dicarbohydrazide 3-dinitromethanide-1,2,4-triazolone (12). Yellow solid (0.84 g, 95%); ^{1}H NMR (DMSO-d6): δ 11.4 (br, 1H), 11.1 (br, 1H), 8.0 (br, 10H) ppm; ^{13}C NMR (DMSO-d6): δ 157.3, 155.9, 139.4, 124.4 ppm; ^{15}N NMR(DMSO-d6): δ −21.9, −72.2, −112.2, −237.5, −297.9 ppm; IR (KBr): ṽ 3346, 3112, 1664, 1570, 1479, 1460, 1212, 1136, 1070, 978, 799, 762 cm^{-1}; elemental analysis, Calcd (%) for $C_7H_{15}N_{13}O_9$ (425.28): C: 19.77; H: 3.56; N: 42.82; Found, C: 19.69; H: 3.55; N: 42.04.

Conflicts of interest

The authors declare no conflict of interest

Acknowledgements

References

1 J. P. Agrawal and R. D. Hodgson, Organic Chemistry of Explosives, John Wiley & Sons Ltd, Copyright 2007.
2 X. Mei, H. Yang, X. Li, Y. Li and Y. Cheng, *Propellants, Explos, Pyrotech*, 2015, **40**, 526–530.
3 S. Date, T. Sugiyama, N. Itadzu and S.Nishi, *Propellants, Explos, Pyrotech*, 2011, **36**, 51–56.
4 A. Tanver, M. Huang and Y. Li, *RSC Adv*, 2016, **6**, 49101–49112.
5 W. Pang, X. Fan, F. Zhao, H. Xu, W. Zhang, H. Yu, Y. Li, Liu, W. Xie and N. Yan, *Propellants, Explos, Pyrotech*, 2013, **38**, 852–859.
6 Q. Yan, M. Gozin, F. Zhao, A. Cohen and S. Pang, *Nanoscale*, 2016, **8**, 4799–4851.
7 X. Zhang, L. Shen, Y. Luo, R. Jiang, H. Sun, J. Liu, T. Fang, H. Fan and Z. Liu, *Ind. Eng. Chem. Res.*, 2017, **56**, 2883–2888.
8 W. Zhang, J. Zhang, M. Deng, X. Qi, F. Nie and Q. Zhang, *Nat. Commun*, 2017, **8**, 181.
9 Y. Wang, Y. Liu, S. Song, Z. Yang, X. Qi, K. Wang, Y. Liu, Q. Zhang, Y. Tian, *Nat. Commun*, 2018, **9**, 2444.
10 Y. Liu, J. Zhang, K. Wang, J. Li, Q. Zhang, and J. M. Shreeve, *Angew. Chem. Int. Ed.*, 2016, **55**, 11548–11551.
11 Z. Xu, G. Cheng, H. Yang, X. Ju, P. Yin, J. Zhang, and J. M. Shreeve, *Angew. Chem. Int. Ed*, 2017, **56**, 5877 −5881.
12 P. Yin, J. Zhang, L. A. Mitchell, D. A. Parrish and J. M. Shreeve, *Angew. Chem. Int. Ed*, 2016, **55**, 12895 −12897.
13 P. Yin, J. Zhang, G. H. Imler, D. A. Parrish and J. M. Shreeve, *Angew. Chem. Int. Ed*, 2017, **56**, 8834 −8838.
14 A. J. Bellamy and S. J. Ward, *Propellants, Explos, Pyrotech*, 2002, **27**, 49 − 58.
15 P. Yin, L. A. Mitchell, D. A. Parrish, and J. M. Shreeve, *Chem. Asian J.* 2017, **12**, 378 − 384.
16 R. D. Schmidt, G. S. Lee, P. F. Pagoria and A. R. Mitchell, *J. Heterocyclic. Chem*, 2001, **38**, 1227 -1230.
17 X. Zhao, C. Qi, L. Zhang, Y. Wang, S. Li, F. Zhao and S. Pang, *Molecules,* 2014, **19**, 896-910.
18 T. D. Tran, P. F. Pagoria, D. M. Hoffman, J. L. Cutting, R. S. Lee and R. L. Simpson, 33rd International Annual Conference on ICT on Energetic Materials-Synthesis, Production and Application, Karlsruhe, Germany, 2002, June 25-28.
19 W. Xu, C. An, J. Wang, J. Dong, and X. Geng, *Propellants, Explos, Pyrotech*, 2013, **38**, 136 − 141.
20 H. Gao and J. M. Shreeve, *Chem. Rev*, 2011, **111**, 7377–7436.
21 A. A. Dippold and T. M. Klapötke, *Chem. Eur. J*, 2012, **18**, 16742 − 16753.
22 A. A. Dippold and T. M. Klapötke, *J. Am. Chem. Soc*, 2013, **135**, 9931–9938.
23 V. Thottempudi, H. Gao and J. M. Shreeve, *J. Am. Chem. Soc*. 2011, **133**, 6464–6471.
24 V. Thottempudi and J. M. Shreeve, *J. Am. Chem. Soc*. 2011, **133**, 19982–19992.
25 C. H. Lim, S. H. Hong, K. H. Chung, J. S. Kim and J. R. Cho, *Bull. Korean Chem. Soc*, 2008, **29**, 1415–1417.
26 T. M. Klapötke and F. X. Steemann, *Propellants, Explos, Pyrotech*, 2010, **35**, 114–129.
27 X. Zhao, S. Li, Y. Wang, Y. Li, F. Zhao and S. Pang, *J. Mater. Chem. A*, 2016, **4**, 5495–5504.
28 H. Huang, Y. Li, J. Yang, R. Pan and X. Lin, *New J. Chem*, 2017,**41**, 7697-7704.
29 The UN recommendations on the transport of dangerous goods, impact: insensitive > 40 J, less sensitive ⩾ 35 J, sensitive ⩾ 4 J, very sensitive ⩽ 3 J. Friction: insensitive > 360 N, less sensitive = 360 N, 80 N < sensitive < 360 N, very sensitive < 80 N, extremely sensitive < 10 N.
30 J. Zhang, L. A. Mitchell, D. A. Parrish, and J. M. Shreeve, *J. Am. Chem. Soc*. 2015, **137**, 10532−10535.
31 P. Yin, L. A. Mitchell, D. A. Parrish and J. M. Shreeve, *Angew. Chem. Int. Ed.*, 2016, **55**, 14409 −14411.
32 P Yin, D. A. Parrish, and J. M. Shreeve, *J. Am. Chem. Soc*, 2015, **137**, 4778–4786.
33 J. Zhang, Q. Zhang, T. T. Vo, D. A. Parrish, and J. M. Shreeve, *J. Am. Chem. Soc*, 2015, **137**, 1697−1704.
34 P. Politzer and J. S. Murray, *J. Mol. Model*, 2015, **21**, 25−36.
35 E. R. Johnson, S. Keinan, P. M. Sánchez, J. C. García, A. J. Cohen and W. Yang, *J. Am. Chem. Soc*, 2010, **132**, 6498−6506.
36 M. A. Spackman and D. Jayatilaka, *Cryst. Eng. Comm*, 2009, **11**, 19−32.
37 Z. Zeng, H. Gao, B. Twamley and J. M. Shreeve, *J. Mater. Chem*, 2007, **17**, 3819−3826.

38 J. Zhang, S. Dharavath, L. A. Mitchell, D. A. Parrish, and J. M. Shreeve, *J. Am. Chem. Soc*, 2016, **138**, 7500−7503.

39 H. Li, F. Zhao, B. Wang, L. Zhai, W. Lai and N. Liu, *RSC Adv*, 2015, **5**, 21422–21429.

40 Y. Li, H. Huang, X. Lin, R. Pan and J. Yang, *Dalton Trans*, 2016, **45**, 15644–15650.

41 A. A. Dippold and T. M. Klapötke, *Z. Anorg. Allg. Chem*. 2011, **637**, 1453–1457.

37 R. Haiges and K. O. Christe, *Inorg. Chem*. 2013, **52**, 7249−7260.

42 T. M. Klapötke, N. Mayr, J. Stierstorfer and M. Weyrauther, *Chem. Eur. J*, 2014, **20**, 1410 – 1417.

43 Frisch, M. J.; Trucks, G. W.; Schlegel, H. G.; Scuseria, G. E.; Robb, M. A.; Montgomery, J. A., Jr; Vreven, T.; Kudin, K. N.; Burant, J. C.; Millam, J. M.; Iyengar, S. S.; Tomasi, J.; Barone, V.; Mennucci, B.; Cossi, M.; Scalmani, G.; Rega, N.; Petersson, G. A.; Nakatsuji, H.; Hada, M.; Ehara, M.; Toyota, K.; Fukuda, R.; Hasegawa, J.; Ishida, M.; Nakajima, T.; Honda, Y.; Kitao, O.; Nakai, H.; Klene, M.; Li, X.; Knox, J. E.; Hratchian, H. P.; Cross, J. B.; Bakken, V.; Adamo, C.; Jaramillo,J.; Gomperts, R.; Stratmann, R. E.; Yazyev, O.; Austin, A. J.; Cammi, R.; Pomelli, C.; Ochterski, J. W.; Ayala, P. Y.; Morokuma, K.; Voth, G. A.; Salvador, P.; Dannenberg, J. J.; Zakrzewski, V. G.; Dapprich, S.; Daniels, A. D.; Strain, M. C.; Farkas, O.; Malick, D. K.; Rabuck, A. D.; Raghavachari, K.; Foresman, J. B.; Ortiz, J. V.; Cui, Q.; Baboul, A. G.; Clifford, S.; Cioslowski, J.; Stefanov, B. B.; Liu, A. L. G.; Piskorz, P.; Komaromi, I.; Martin, R. L.; Fox, D. J.; Keith, T.; Al-Laham, M. A.; Peng, C.; Nanayakkara, A.; Challacombe, M.; Gill, P. M. W.; Johnson, B.; Chen, W.; Wong, M.; Gonzalez, C.; Pople, J. A. Gaussian 03, revision D.01; Gaussian, Inc.: Wallingford, CT, 2004.

44 Lu, T.; Chen, *F. J. J. Comput. Chem*, 2012, **33**, 580−592.

45 Humphrey, W.; Dalke, A.; Schulten, *K. J. Mol. Graphics Modell*. 1996, **14**, 33−38.

46 Wolff, S. K.; Grimwood, D. J.; McKinnon, J. J.; Turner, M. J.; Jayatilaka, D.; Spackman, M. A. CrystalExplorer, version 3.1; University of Western Australia: Crawley, Australia, 2012.

47 Bruker SAINT (SADABS), v2008/1; Bruker AXS Inc.: Madison, Wisconsin, 2008.

48 Bruker SHELXTL, v2008/1; Bruker AXS Inc.: Madison, Wisconsin, 2008.